Improved Delineation of Saline Groundwater by Airborne Electromagnetics

Klaus-Peter Sengpiel
Federal Institute for Geosciences and Natural Resources (BGR)
Postfach 510153, D–30631 Hannover, Germany

Measuring principles

For several decades d.c. resistivity soundings have been used to provide valuable information for groundwater surveys. Only very recently have electromagnetic (EM) induction methods begun to provide similar standards of data evaluation, particularly in resolving resistivities and thicknesses of a layered halfspace from survey data. EM methods have the advantage that neither transmitters nor receivers require galvanic contact with the ground. Therefore, they can be moved during measurement and operated at considerable height above ground surface. For helicopter applications, transmitters and receivers are housed in a towed missile ("bird"), where they are spaced only a few meters apart. The bird is flown at a height of about 30 m above ground, providing a depth of investigation of up to 150 m with standard equipment.

BGR operates a helicopter-borne Dighem-III system as shown in the sketch (Fig. 1). The system is flown at a speed of up to 150 km/h. The primary magnetic field oscillates at three frequencies simultaneously, normally 380, 3 600 and 32 000 Hz, in order to induce current systems which are centered at different depths. The current density is a function of the ground conductivity; therefore, good conductors such as saltwater-bearing aquifers provide stronger signals than freshwater aquifers and much stronger signals than dry sand. The signal is the sum of the (secondary) magnetic fields of all induced currents at one frequency. In Fig. 1 the secondary field comes from the three layers and the conductor; the signal is transformed into a voltage by means of a receiver coil.

It should be noted that the induced currents and their magnetic fields in general have a phase shift relative to the phase of the primary field (unlike d.c. fields). Thus, two values are measured at each frequency: the inphase (real) field component R and the out-of-phase (imaginary) field component Q. The R and Q values of all frequencies are sampled 4 to 10 times a second together with positioning data (GPS coordinates, barometric and radar altitudes) and data from the other geophysical methods applied with the BGR geophysics helicopter, namely magnetics (total geomagnetic field) and gamma-ray spectrometry (256 energy channels). All data are stored on magnetic tape (cassette) and on chart paper. A sampling rate of 4/sec corresponds to a sampling distance of about 10 m on the flight line.

Inversion of measured EM data into ground parameters

The measured data originate from ground in which the resistivity distribution is unknown. When beginning evaluation, it is common practice to assume that the ground is uniform around the measurement site, i.e. to use the homogeneous halfspace model. This leads to the "apparent" resistivity ρ_a (or apparent conductivity $\sigma_a = 1/\rho_a$) which is obtained for each measuring frequency.

Over the last 20 years, the airborne EM method has proved to be a very useful tool for mapping the lateral (apparent) resistivity distribution both in detail and at high survey speed (Fraser, 1978). Besides ρ_a, a second parameter (D_a) can be determined from the two input values R and Q, where D_a is the (apparent) distance between the coil system and the surface of the halfspace model. D_a can be compared with the flight altitude of the EM bird and thus can yield preliminary information on the vertical resistivity distribution in the ground. Furthermore, ρ_a and D_a can be used to calculate a depth value z^* called the centroid depth (Sengpiel, 1988), which is a measure of the depth of the center of the induced current system.

The parameters ρ_a and z^*, calculated for a great number of frequencies, define the sounding curve $\rho_a(z^*)$ shown in Fig. 2. This curve is obtained for the three-layer (step) model $\rho(z)$, where $\rho_1 = 200$ Ωm, $\rho_2 = 20$ Ωm, $\rho_3 = 1000$ Ωm, and the layer thicknesses are $d_1 = 30$ m, $d_2 = 40$ m, and $d_3 = \infty$. This sounding curve is closely related to the model, at least in the range of the upper two layers, while the ρ-value of the third layer is only approached very gradually by the curve.

In reality, with only the three frequencies f_1, f_2, f_3 available as indicated in Fig. 2 by asterisks on the curve, we obtain merely a short piece of the sounding curve, yielding the approximate resistivities in the depth range of about 20 to 60 m. An improvement of the inversion capabilities was achieved in 1993 when BGR started using its newly developed "Automatic inversion of AEM data into multilayer parameters" (Sengpiel et al., 1994). This evaluation procedure uses the sounding parameters ρ_a and z^* to develop an individual start model for each set of survey data. An iteration process based on a Marquardt inversion varies the model parameters until an optimum fit is achieved between the survey data and the calculated field data for the inversion model. It is only necessary to define the number of layers of the inversion model. This number can be derived from the $\rho_a(z^*)$ sounding curve or from other information, especially drilling results. With good quality field data, the inversion process can provide accurate step model parameters. In Fig. 2, this case applies for inversion model (1), calculated for $\delta =$ 0.01 %, where δ is the residual misfit between model data and (theoretical) survey data. The value δ is adjusted according to the accuracy of the survey data. Allowing for a typical misfit of $\delta \approx 10$ % for survey data, the accuracy of the inversion parameters is reduced; this affects mainly the lower and less conductive layers (layer 3 in Fig. 2). The choice of the number of layers (N) is not critical, provided N is equal or greater than the true number of significant layers.

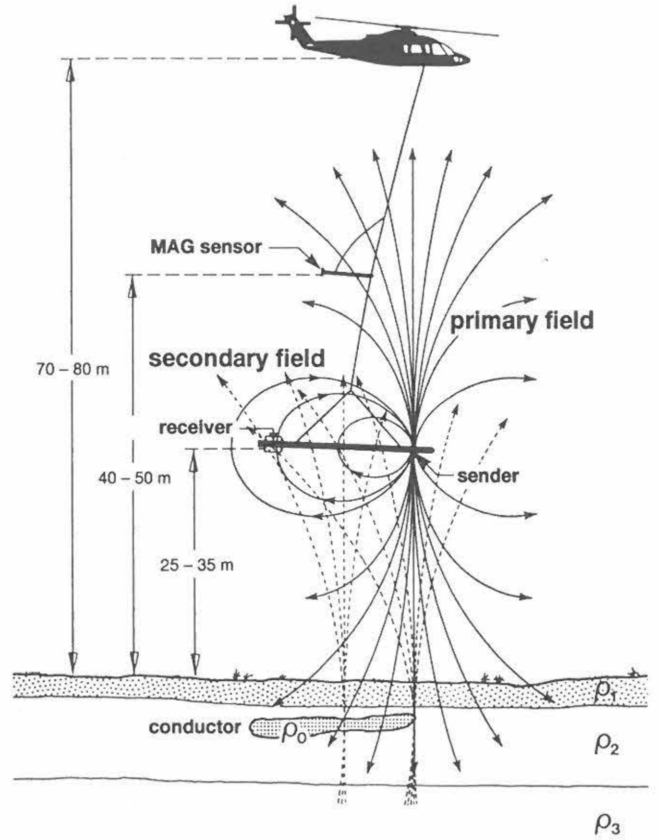

Fig. 1: Sikorsky S 76 B helicopter carrying the EM and magnetometer sensors at the indicated elevations above ground. Geometry of the transmitted primary magnetic field (dipole field) inducing currents in the conductive parts of the ground. Sketch of the secondary magnetic fields of these currents flowing in the three layers (ρ_1, ρ_2, ρ_3) and the conductor (ρ_0); a small portion of the secondary field passes through the receiver coil.

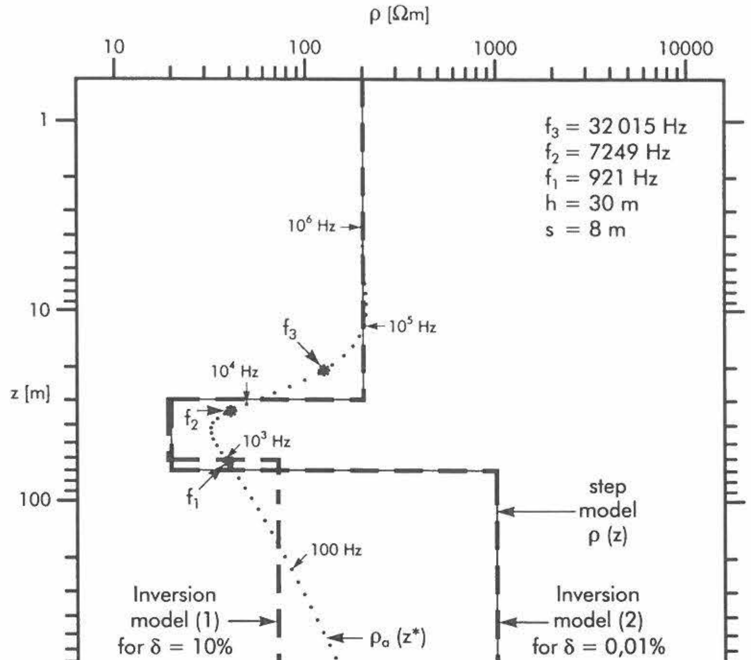

Fig. 2: ρ/z diagram showing resistivities ρ and thicknesses d of a three-layer model ρ(z), where ρ_1 = 200, ρ_2 = 20, ρ_3 = 1000 Ωm, d_1 = 30, d_2 = 40 m, and the results of different inversion methods:
- The sounding curve ρ_a (z*) obtained when a large number of frequencies is used,
- the perfect inversion (model 1) using perfect survey data (δ = 0.01 %),
- a less accurate inversion (model 2) simulating imperfect survey data (δ = 10 %).

Presentation of survey results

Apparent resistivity values and layer resistivities are assigned different colours and presented in the form of coloured contour maps using conventional gridding and plotting routines. Low resistivities are normally plotted in red and orange, high resistivities in blue, and intermediate values in yellow and green. Fig. 3 is an example of an apparent resistivity map using different shades of grey, dark grey for low resistivities. It is possible to print black isolines on a (coloured) layer resistivity map to indicate the thickness of a selected layer or the elevation above sea level of its upper boundary.

As is well known, the contouring process can smooth out small-scale details. A fully detailed representation of the survey results is accomplished by means of "vertical resistivity sections" (VRS) which are based on the inversion results ρ_i and d_i for all layers ($i = 1,2,...,N$) at each measuring site along a flight line. Fig. 4 shows examples of such VRS where the original colours of ρ_i are reproduced in grey by the copying process. The d_i values determine the layer boundaries which are related to the topographic elevation (m above sea level) at each measuring site, given on the vertical axis of the plots (left side). The colour (or grey) code representing the layer resistivities below a measuring site is plotted in form of a very narrow vertical column. All these columns, plotted side by side, represent a continuous resistivity distribution along the flight line. The thin line above the topographic relief shows the flight path of the EM sensor. Fig. 4 represents only the lower parts of the original VRS; the upper part normally contains the measured R and Q values along the line and data from the two other methods, such as the magnetic anomalies and the total gamma radiation (in uranium equivalents).

Examples of groundwater investigation results

In 1992 and 1993 BGR conducted several helicopter surveys in Namibia to support groundwater investigations. In this semi-arid to arid region, saline groundwater was a common problem, not only in coastal areas but almost everywhere.

A special challenge for geophysics was an investigation in the Namib Desert south of the important port of Walvis Bay, where the recharge of freshwater resources is smaller than the increasing demand. The survey area has a maximum extent of 100 km E–W and 90 km N–S and is almost completely covered by dune sand with a relief of up to 100 m. Fig. 3 shows the apparent resistivity distribution in the whole area at an drastically reduced scale (approx. 1:710 000) and at a measuring frequency of 921 Hz (Sengpiel & Siemon, 1995). Although the NNW trending dune valleys and ridges are still recognizable, the resistivity pattern of the bedrock beneath is also shown and reveals a number of crossing structures. The high resistivities of the crystalline basement (gneiss, granite, schist, quartzite) are indicated by the bright area in Fig. 3, ("basement"), where the sediment cover is thin. Outcropping basement is also found in the bright patches N and S of PC 6, while the broad, light grey strip in the W is due to the sand cover. The basement is generally overlain by the (conductive) Tsondab Sandstone (Ward, 1987) which is represented by the dark grey in Fig. 3 ("TS"). The lowest resistivities (around 1 Ωm) appear black.

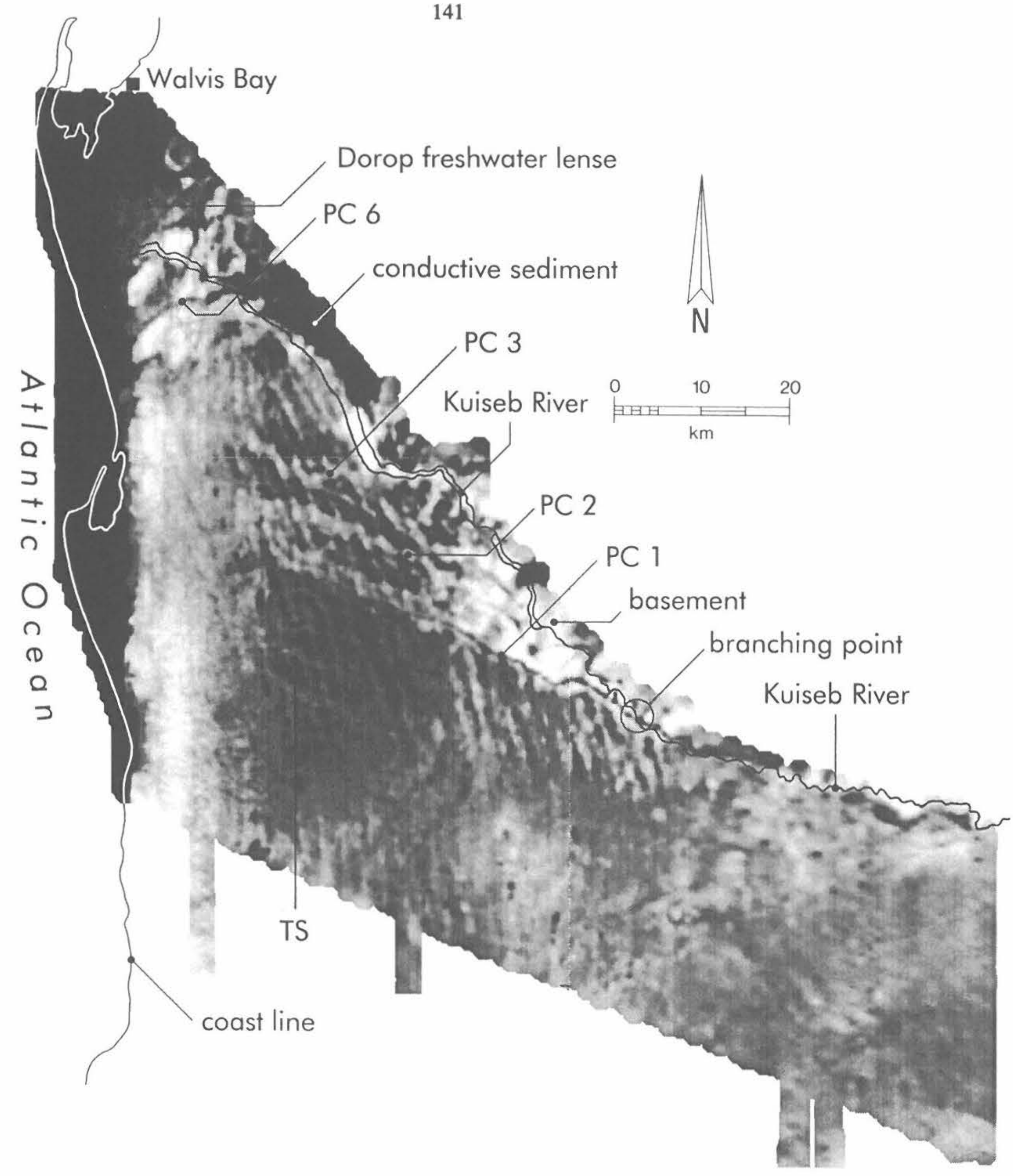

Fig. 3: Grey scale representation of apparent resistivity ρ_a (at 921 Hz) in the Kuiseb Dunes area of Namibia, showing mainly the resistivity pattern of the bedrock below a thick sand cover; only the NNW-trending features originate from dune ridges and valleys. The structures PC 1 to PC 6 were identified as palaeochannels of the Kuiseb River, which has shifted its course stepwise from PC 1 to the north. The palaeochannels are cut into basement rock (light-coloured areas) and/or conductive Tsondab Sandstone (medium dark areas, TS). The black area along the coastline indicates highly conductive saltwater intrusion. Along its eastern edge it is overlain by freshwater pockets (subtle dark-grey features).

Along the coastline the black areas indicate open sea water and sea-water intrusions into the sandy lowlands in the NW. Pockets of freshwater can be detected as subtle features which overlie the saltwater, as is the case for the well-known Dorop freshwater lens (Fig. 3) and similar, smaller pockets along the inland boundary of the saltwater intrusion. The Tsondab Sandstone Formation is cut by several WNW trending structures (PC1, PC2, PC3). The most prominent one is PC 1 which branches off the present-day Kuiseb river at a point indicated in Fig. 3 and continues as a thin dark line in WNW direction. A number of exploration boreholes have shown that these structures are former valleys ("palaeochannels") deeply incised into the Tsondab sandstone and/or the basement. These valleys are filled with fine-grained sediments and fresh or brackish water. The water potential of the investigated palaeochannels amounts to about 100 Mm^3 of brackish and 280 Mm^3 of fresh groundwater (Plöthner, 1995).

The ρ_a map of Fig. 3 is accompanied by more than 12 000 line km of vertical resistivity sections for four or five layer models. Fig. 4 is a grey copy of three coloured VRS which extend over 20 line km, parallel to the north-western coast across the Dorop freshwater lens indicated in Fig. 3. Note that the grey scale of Fig. 4 is different from that of Fig. 3. The Dorop aquifer has a formation resistivity around 30 Ωm, overlies strongly saline water (~ 1 Ωm), and thins out towards the coast (from bottom to top in Fig. 4). The first layer (dark) represents the highly resistive sand cover ($\rho_1 > 1000\ \Omega$m). The boundary between layer 1 and 2 indicates the approximate groundwater table and occurs at 0 m above m.s.l. or somewhat higher.

Finally, Fig. 5 shows two VRS along flight lines (tie lines) which cross the northern part of the Dorop aquifer (line 927.9) and its southern part (line 926.9), both from SE to NW. Besides the known Dorop aquifer, more fresh water is expected in PC 6b (line 927.9 and 926.9) which is separated from the Dorop aquifer by a bedrock high. Above the water table (w.t. in Fig. 5) of PC 6b of the lower VRS there are three layers of somewhat higher resistivity, which are assigned to extremely dry sand (on top) and underlying sand with a residual moisture content. The very steep dip on the flanks of the bedrock highs is probably an apparent feature rather than a real one. It should be borne in mind that the one-dimensional layer model only deals with vertical changes in ρ, not lateral ones. While a gradual lateral change can be accommodated by the inversion process, higher gradients cannot, and in some cases produce fictitious vertical boundaries.

Conclusions

In addition to the survey results presented here, many thousand line km were surveyed and evaluated using the techniques described above. This demonstrates that groundwater salinity can be reliably mapped in three dimensions by airborne EM, preferably in areas where unconsolidated sediments prevail. The water table can be determined under favourable conditions, i.e. if there is a significant resistivity contrast between unsaturated cover and the aquifer. The airborne survey should be followed immediately by a test drilling program; a few boreholes may provide the key to understanding the relationship between resistivity and hydrogeology of a whole region. BGR is trying to increase the resolution and the reliability of the survey results by the development of a new five-frequency EM sensor, which is expected to be in operation in 1996.

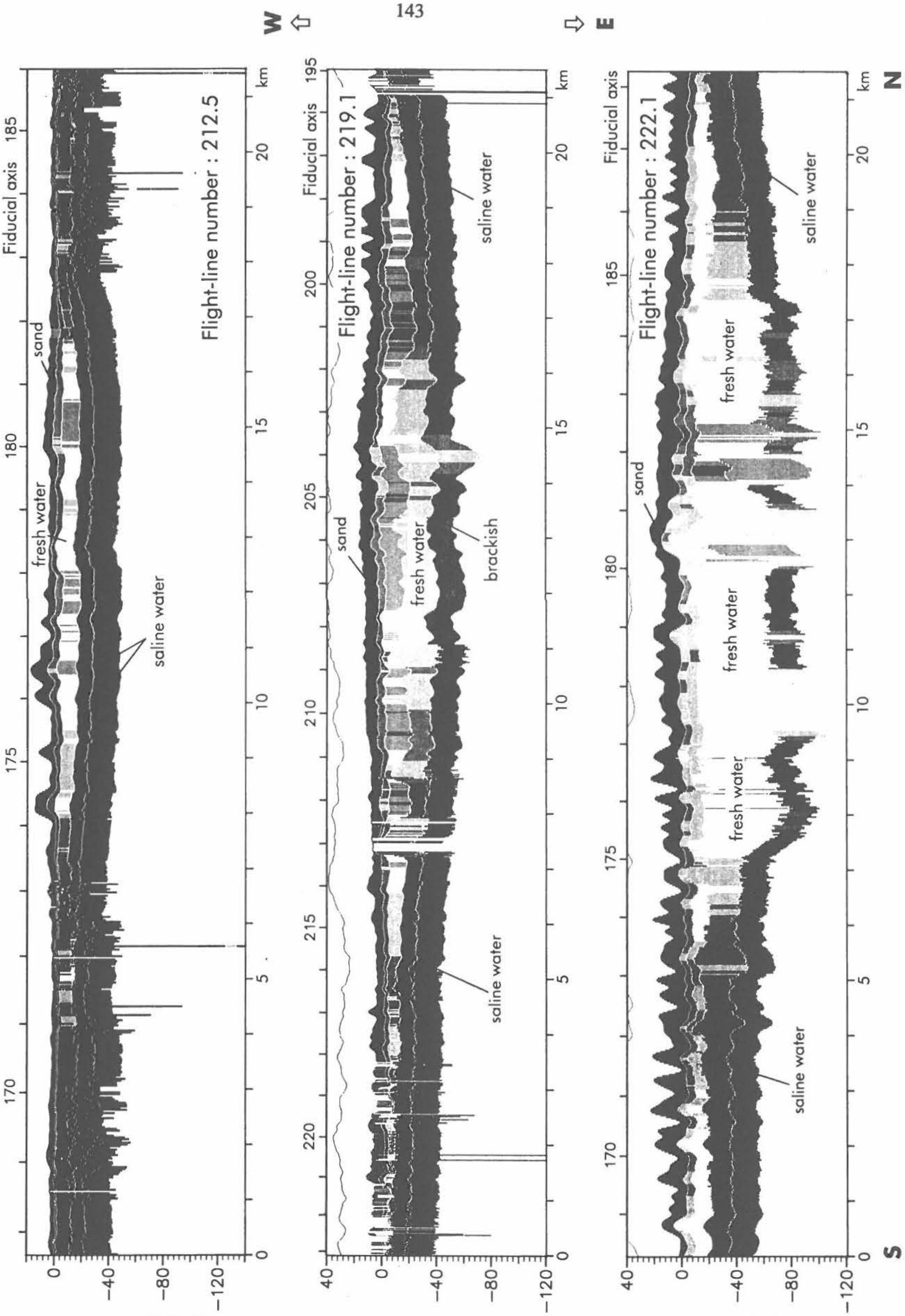

Fig. 4: Vertical resistivity sections (VRS) from airborne EM data provide a three-dimensional picture of a freshwater lens surrounded by saline water in a sandy environment (Dorop freshwater lens in Fig. 3). Flight lines are oriented N–S; line 212.5 is the westernmost, situated about 4 km E of the coast, the others follow 2.4 km and 3.6 km further inland. Resistivities are represented by grey shading and correspond to the types of groundwater indicated, known from drillings.

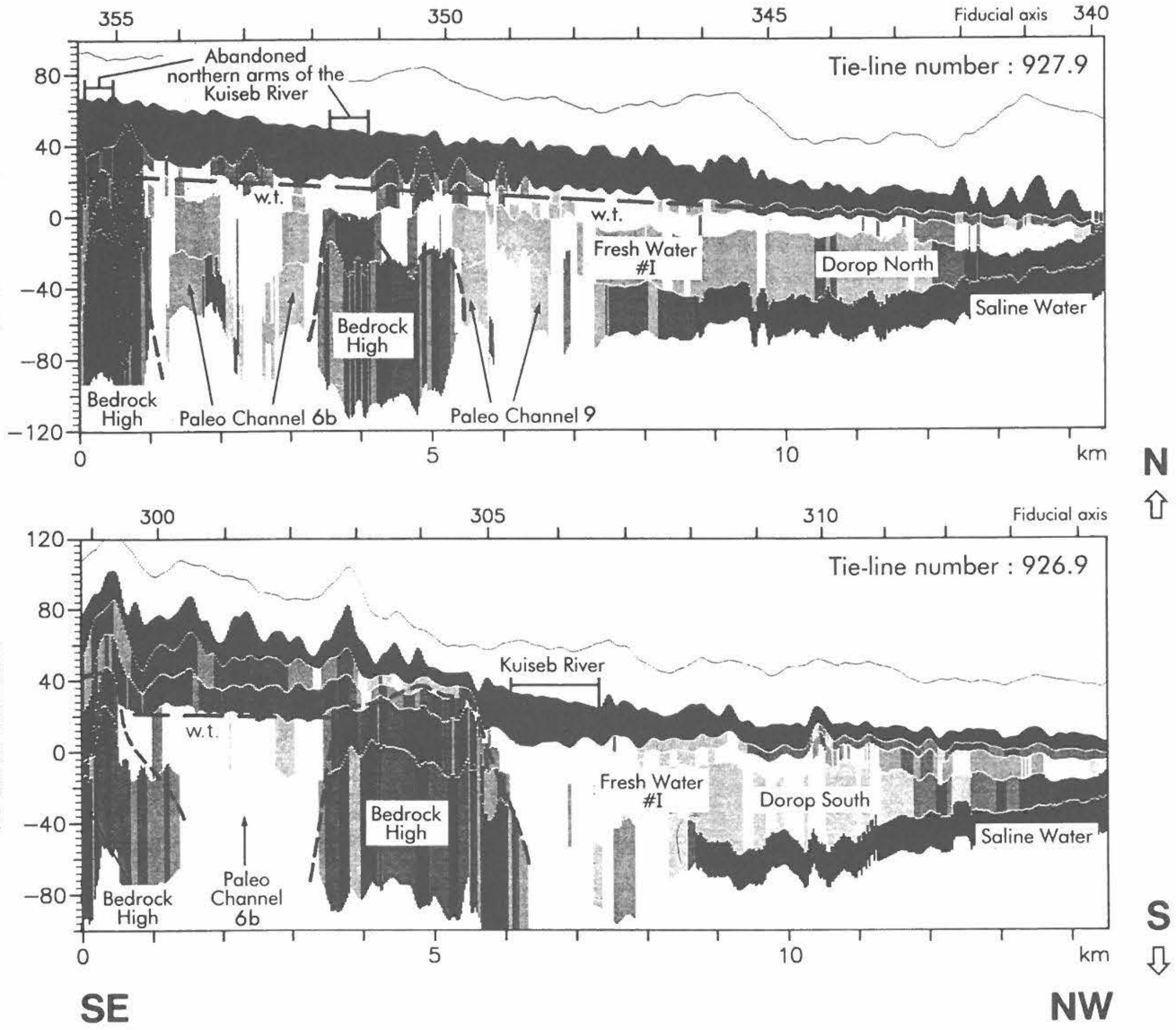

Fig. 5: VRS for SE–NW tie-lines showing the Dorop aquifer (see Figs. 3 & 4), the underlying "saline wedge", and the bordering bedrock high SE of Dorop. Another freshwater aquifer (PC 6b) can be identified between bedrock flanks of higher resistivity.

References

FRASER, D.C., 1978: Resistivity mapping with an airborne multicoil electromagnetic system. - Geophysics, v. 43, pp. 144-172.

PLÖTHNER, D., 1995: Status report of the German-Namibian groundwater exploration project (GNGEP), Jan. 1994 - Feb. 1995. - BGR archives no. 112 764 (unpublished), Hannover.

SENGPIEL, K.-P., 1988: Approximate inversion of airborne EM data from a multilayered ground. - Geophysical Prospecting 36, pp. 446-459.

SENGPIEL, K.-P., FLUCHE, B., LENZ, R., RÖTTGER, B., AND VOSS, W., 1994: Automatic inversion of AEM data into multilayer parameters and its application to groundwater exploration in the Namib Desert. Extended Abstracts Book of the International Meeting in Vienna. EAEG, Zeist.

SENGPIEL, K.-P. & SIEMON, B., 1995: The BGR helicopter survey in the Kuiseb Dune Area (Central Namib Desert) 1992; Interpretation of Geophysical Data. Vol. B-III. BGR archives no. 113 810 (unpublished), Hannover.

WARD, J.D., 1987: The Cenozoic succession in the Kuiseb Valley, Central Namib Desert. Geol. Surv. Namibia Memoir, 9, Windhoek.